

A Green Protocol for the Electrochemical Synthesis of a Fluorescent Dye with Antibacterial Activity from Imipramine Oxidation

Zahra Souri

Yazd University

Mahmood Masoudi Khoram

Bu-Ali Sina University

Davood Nematollahi (✉ nemat@basu.ac.ir)

Bu-Ali Sina University

Mohammad Mazloun-Ardakani

Yazd University

Hojjat Alizadeh

Rooyana Veterinary Laboratory

Research Article

Keywords: Imipramine, Electrochemical oxidation, Electrochemical dimerization, Cyclic voltammetry, Controlled potential coulometry, Fluorescence activity, Antibacterial susceptib

Posted Date: November 17th, 2021

DOI: <https://doi.org/10.21203/rs.3.rs-1044924/v1>

License:  This work is licensed under a Creative Commons Attribution 4.0 International License.

[Read Full License](#)

Version of Record: A version of this preprint was published at Scientific Reports on March 22nd, 2022. See the published version at <https://doi.org/10.1038/s41598-022-08770-4>.

1 A Green Protocol for the Electrochemical 2 Synthesis of a Fluorescent Dye with 3 Antibacterial Activity from Imipramine 4 Oxidation

5 Zahra Souri¹, Mahmood Masoudi Khoram², Davood Nematollahi^{*2}, Mohammad Mazloum-Ardakani¹, Hojjat Alizadeh³

6 ¹Department of Chemistry, Faculty of Science, Yazd University, Yazd, Iran. ²Faculty of Chemistry, Bu-Ali Sina University, Hamedan, Iran.
7 Zip Code 65178-38683. ³Rooyana Veterinary Laboratory, Saqqez, Kurdistan, Iran. E-mail: nemat@basu.ac.ir. Fax: 0098 - 813- 8257407, Tel:
8 0098 - 813- 8282807

9 ABSTRACT

10 Electrochemical oxidation of imipramine (IMP) has been studied in aqueous solutions by cyclic voltammetry and
11 controlled-potential coulometry techniques. Our voltammetric results show a complex behavior for oxidation of
12 IMP at different pH values. In this study, we focused our attention on the electrochemical oxidation of IMP at a
13 pH of about 5. Under these conditions, our results show that the oxidation of IMP leads to the formation of a
14 unique dimer of IMP (DIMP). The structure of synthesized dimer is fully characterized by UV-visible, FTIR, ¹H
15 NMR, ¹³C NMR and mass spectrometry techniques. It seems that the first step in the oxidation of IMP is the
16 cleavage of the alkyl group (formation of IMPH). After this, a domino oxidation-hydroxylation-dimerization-
17 oxidation reaction, converts IMPH to (*E*)-10,10',11,11'-tetrahydro-[2,2'-bidibenzo[b,f]azepinylidene]-
18 1,1'(5*H*,5'*H*)-dione (DIMP). The synthesis of DIMP is performed in an aqueous solution under mild conditions,
19 without the need for any catalyst or oxidant. Based on our electrochemical findings as well as the identification
20 of the final product, a possible reaction mechanism for IMP oxidation has been proposed. Conjugated double
21 bonds in the DIMP structure cause the compound to become colored with sufficient fluorescence activity
22 (excitation wave-length 535 nm and emission wave-length 625 nm). Moreover, DIMP has been evaluated for in
23 vitro antibacterial. The antibacterial tests indicated that DIMP showed good antibacterial performance against

24 all examined gram-positive and gram-negative bacteria (*Staphylococcus aureus*, *Bacillus cereus*, *Escherichia coli*
25 and *Shigella sonnei*).

26 **Keywords:** Imipramine; Electrochemical oxidation; Electrochemical dimerization; Cyclic voltammetry; Controlled-
27 potential coulometry; Fluorescence activity; Antibacterial susceptibility.

28 Introduction

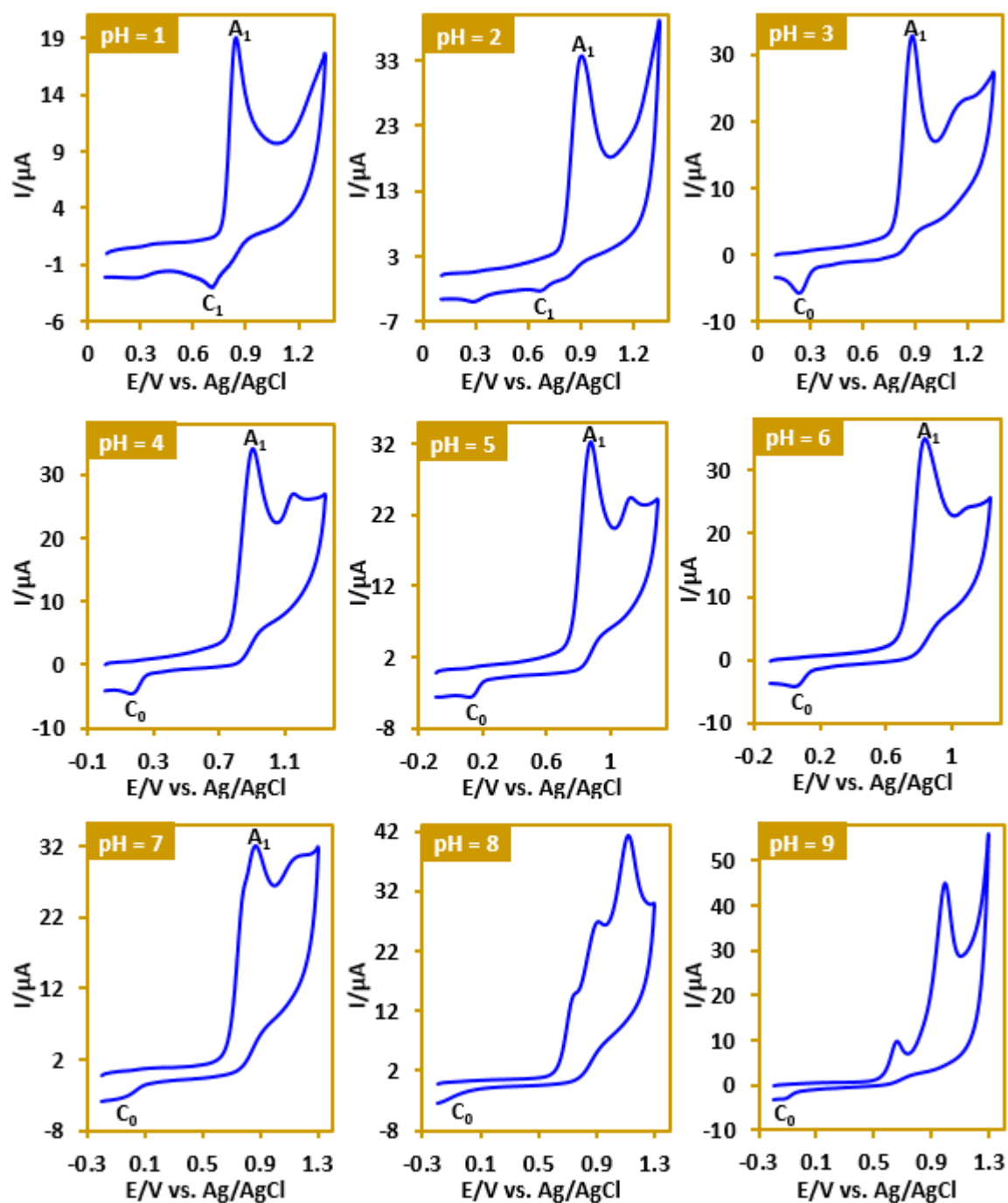
29 Dibenzazepines, as electron-rich compounds, are one of the most important organic substances that have
30 received much attention in academic and technological research.¹⁻³ These compounds have been known since
31 1899 when Tille and Holzinger synthesized 10,11-dihydrodibenzo[b,f]azepine.^{4,5} These compounds can serve as
32 photoactive and electroactive materials in molecular electronics,⁶ electrogenerated chemiluminescence,⁷
33 efficient nonlinear optical materials,⁸ dye-sensitized solar cells (DSSCs),⁹⁻¹¹ and organic light-emitting diodes
34 (OLEDs).¹² In addition, dibenzazepines having N–H bond have attracted much attention because compounds
35 with Ar₂NH structure have always been the central structure in many drugs.^{13,14} Due to the great interest in
36 dibenzazepine derivatives, many synthetic procedures have been developed for such compounds including, the
37 dehydrogenation of iminobibenzyls,^{15,16} the rearrangement of arylindoles¹⁷ and metal catalyzed synthesis.^{18,19}
38 The above methods have several disadvantages such as: using transition metal and toxic chemical reagent,
39 require prefunctionalized substrates, produce undesired toxic side products, heavy metal waste, high
40 temperature, undesirable solvent, functional group-intolerant conditions, low yields and tedious workup.^{18,20-22}
41 Besides these methods, electrochemical methods were also reported for the synthesis of dibenzazepine
42 derivatives.²³⁻²⁶ Electrochemical methods have a wide range of applications in the synthesis of electroactive
43 compounds due to their excellent performance and no need for toxic chemical reagents or expensive noble
44 metals²⁷⁻³³. Moreover, the discovery of new electrode materials, the development of multifunctional practical
45 straightforward equipment, along with bio-renewable solvents will provide in the future robust, general and
46 scale-up electrosynthetic processes compared to traditional methods.³⁴ In this regard, this work has been
47 conducted with the aim of elucidating the electrochemical oxidation of imipramine (**IMP**) and creating a new

48 oxidation pathway for **IMP**. Imipramine is a tricyclic antidepressant used for the treatment of physiological
49 retardation depression, bipolar disorder, dysthymia, hyperactivity disorder.^{35,23} The oxidation mechanism of
50 imipramine has been investigated in only a few studies.³⁵⁻³⁹ This encourages us to do a more complete study on
51 the oxidation pathway of **IMP**. On this subject, the electrocatalytic degradation of imipramine with fluorine-
52 doped β -PbO₂ electrode⁴⁰ and the electrochemical polymerization of imipramine at pH 1.0⁴¹ have recently been
53 studied by us. In order to complete the previous studies,^{40,41} in this work, we investigate the electrochemical
54 oxidation of imipramine in acetate buffer (pH 5.0) and we managed to synthesize a unique dimer (**DIMP**) from
55 this compound. This electroorganic synthesis is performed in one step using efficient and ecofriendly methods
56 in high yield and purity without toxic reagents and solvents at a carbon electrode in an undivided cell. The
57 results show that the first step in the hydroxylation/dimerization of **IMP** is the oxidative dealkylation process.
58 At this point, the alkyl chain separates from the **IMP**. After this step, a series of reactions, including oxidation,
59 hydroxylation, dimerization and oxidation, lead to the synthesis of (*E*)-10,10',11,11'-tetrahydro-[2,2'-
60 bidibenzo[b,f] azepinylidene]-1,1'(5*H*,5'*H*)-dione (**DIMP**) as a fluorescent dye with antibacterial activity.

61 **Results and Discussion**

62 **Mechanistic studies.** Cyclic voltammetry was used to study the redox behavior, pH-dependent properties and
63 electron transfer mechanism of **IMP** in aqueous solution. The pH dependent behavior of **IMP** was investigated
64 by cyclic voltammetry. Fig. 1 shows the cyclic voltammograms of **IMP** at different pH values. As can be seen,
65 the **IMP** exhibits complex and different behaviors. For example, while peak C₁ is present at pH values less
66 than 2, it is not seen at higher pH values. Or peak C₀ is seen in the pH range 3-6 and is gradually removed as
67 the pH increases. On the other hand, while voltammograms show one or two anodic peaks up to pH 6, the
68 number of anodic peaks increases to three as the pH increases further. The fundamental change in the
69 electrochemical behavior of **IMP** in alkaline media may be due to the participation of **IMP** in hydroxylation
70 and/or hydrolysis reactions. These results indicate high complexity in **IMP** oxidation. In previous studies, we
71 have been able to identify some oxidation pathways of this compound.^{40,41} Based on our previous data, peak A₁
72 is attributed to the one-electron oxidation of **IMP** to the corresponding radical cation and peak C₁ is related to

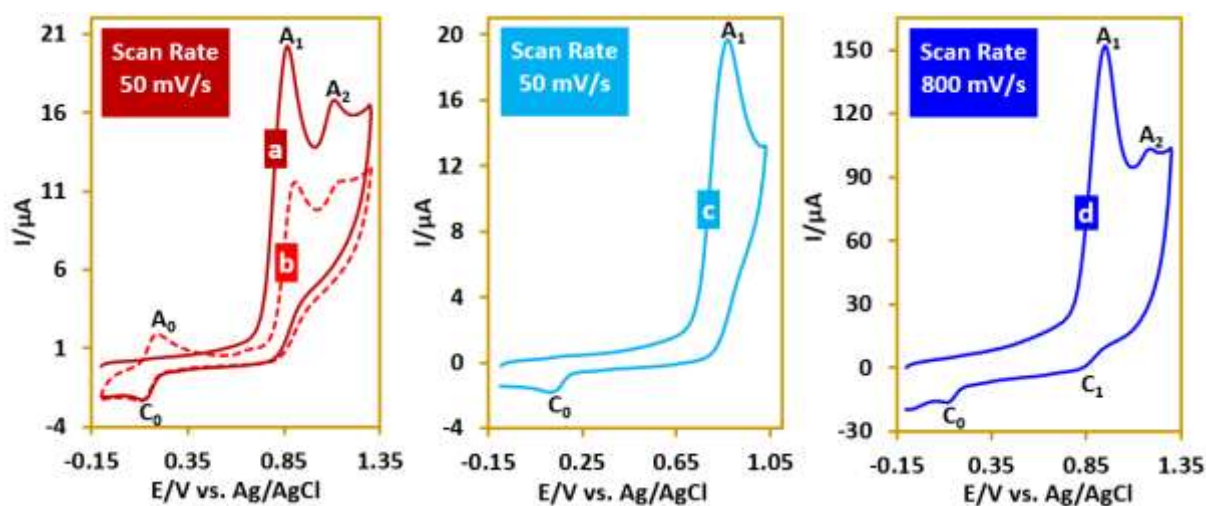
73 the reduction of radical cation to **IMP**.^{40,41} In this work, we pay attention to the behavior of **IMP** in the pH
74 range 3-6.



75

76 **Figure 1.** Cyclic voltammograms of **IMP** (1.0 mM) at glassy carbon electrode in aqueous solutions at different pH
77 values. Scan rate: 100 mV s⁻¹, at room temperature.

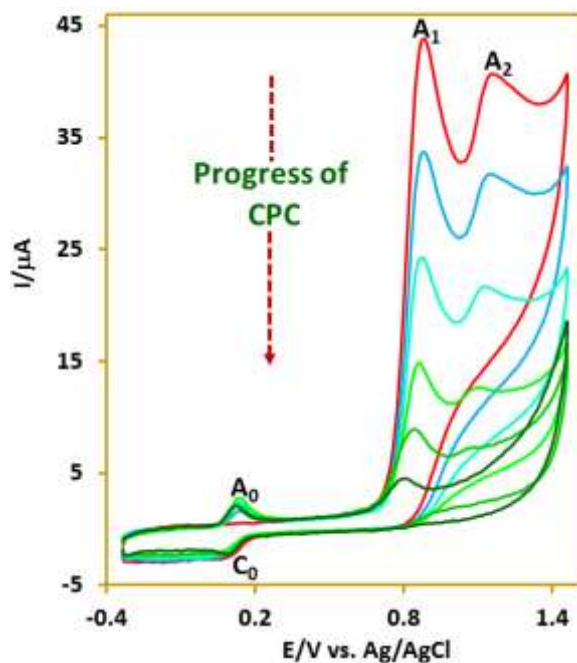
78 Fig. 2, curves a and b shows the first and second cyclic voltammograms of **IMP** in the aqueous solution (pH
 79 5.0) at scan rate of 50 mV s⁻¹. As can be seen, in the first scan, two anodic peaks A₁ and A₂ are observed over the
 80 whole potential range. When the potential is switched to negative potentials, a new reduction peak (C₀) appears at a
 81 potential of 0.13 V vs. Ag/AgCl and in the second cycle, a new anodic peak (A₀) (counterpart of C₀ peak) appears
 82 with E_p of 0.19 V vs. Ag/AgCl. Fig. 2, curve c shows the cyclic voltammogram of **IMP** over the limited potential
 83 range up to 1.0 V vs. Ag/AgCl. The presence of peak C₀ in the voltammogram in these conditions indicates its
 84 independence from peak A₂. Increasing the scan rate in these situations has three important consequences (Fig. 2,
 85 curve d). First, decrease the anodic peak current ratio (I_{pA2}/I_{pA1}). Second, decrease the cathodic-to anodic peak
 86 current ratio (I_{pC0}/I_{pA1}) and third, appearance of the peak C₁.



87
 88 **Figure 2.** Curves a and b: First and second cyclic voltammograms of **IMP** (1.0 mM) at glassy carbon electrode in
 89 water (acetate buffer, $c = 0.2$ M, pH 5.0), at room temperature. Curve c is similar to curve a, but with a more limited
 90 potential range. Curve d is similar to curve a, but at scan rate of 800 mV s⁻¹.

91 In order to better understand the oxidation reaction mechanism at pH 5, here we performed a controlled-
 92 potential coulometry (CPC) experiment to determine the number of transferred electrons and recorded the cyclic
 93 voltammograms of the solution during the coulometry. For this purpose, CPC was carried out in aqueous solution
 94 (80 ml buffer, pH 5.0) containing 0.25 mmol of **IMP** at the potential of 0.85 V versus Ag/AgCl. Fig. 3, shows the
 95 cyclic voltammograms of **IMP** during controlled-potential coulometry. As can be seen, I_{pA1} and I_{pA2} decrease with

96 time (electricity consumption), while I_{pA0} and I_{pC0} increase slightly. Also, the number of electrons exchanged in this
97 experiment was found to be slightly more than 6 electrons.

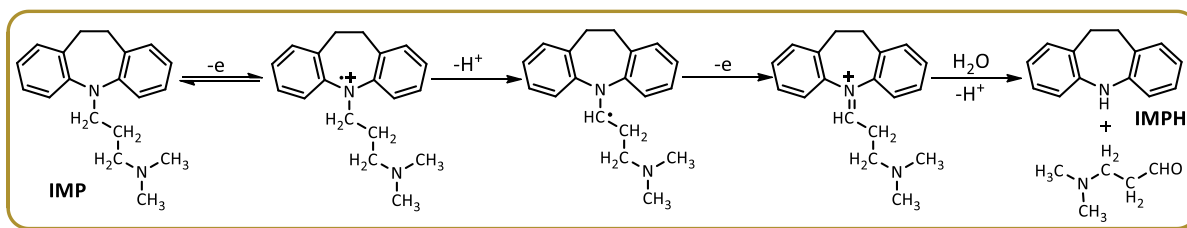


98

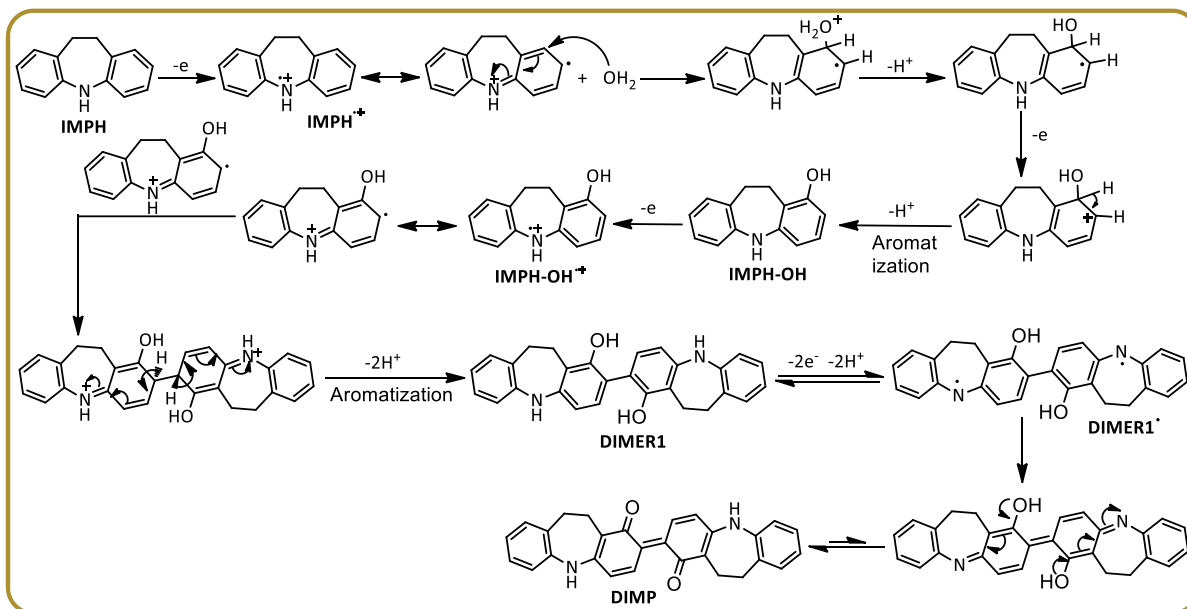
99 **Figure 3.** Cyclic voltammograms of **IMP** (0.25 mmol) during controlled-potential coulometry at +0.85 V versus
100 Ag/AgCl in water (acetate buffer, $c = 0.2$ M, pH 5.0). Scan rate: 50 mV s^{-1} , at room temperature.

101 According to these results together with the spectroscopic data of the isolated product as well as our previous
102 studies,^{40,41} we proposed the following mechanism for the electrochemical oxidation of **IMP** at the pH 5 (Fig. 4).
103 Since the spectroscopic data of the synthetic product show that the alkyl group is not involved the final product, it
104 seems that the first step in the oxidation of **IMP** is the cleavage of the alkyl group from **IMP** (formation of **IMPH**),
105 during an oxidative dealkylation reaction.⁴² In the next step, **IMPH** is oxidized to the corresponding radical cation
106 via a one-electron-transfer process. This compound is converted to **IMPH-OH** after hydroxylation (due to water
107 attack) and then aromatization. In the next step, the **IMPH-OH** is converted to the corresponding radical cation by a
108 one electron transfer process (**IMPH-OH^{•+}**). The reaction of two radical cations of **IMPH-OH** together, followed
109 by aromatization, forms the corresponding dimer (**DIMER1**). Finally, a two-electron oxidation process, together
110 with a rearrangement, converts **DIMER1** to the final product (**DIMP**).

111



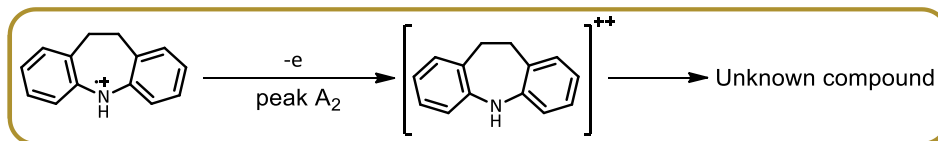
112



113 **Figure 4.** Electrochemical synthesis of **DIMP** by a domino dealkylation-oxidation-hydroxylation-dimerization-
114 oxidation reaction.

115 Based on the available results, peak A_1 and its cathodic counterpart (C_1) (see Fig. 1) are correspond to one-
116 electron oxidation of **IMP** to $\text{IMP}^{\bullet+}$ and vice versa. In this regard, due to the removal of peak A_2 at high scan rates,
117 this peak is related to the over-oxidation of $\text{IMPH}^{\bullet+}$ to IMPH^{2+} (Fig. 5).

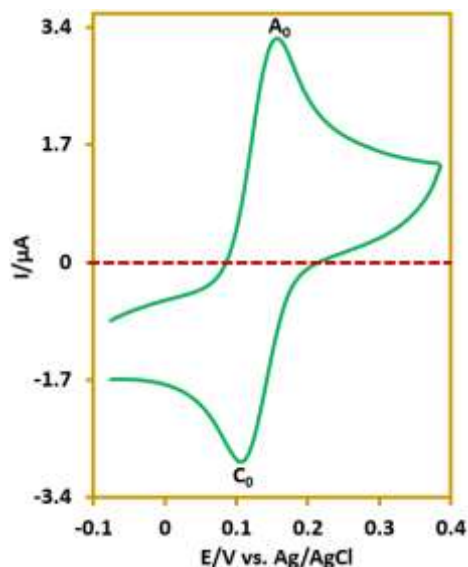
118



119 **Figure 5.** Proposed reaction for generation of peak A_2 .

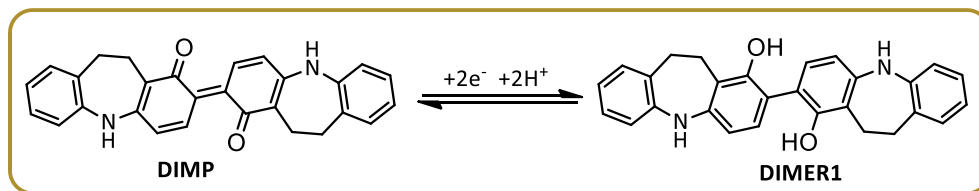
120 In order to determine the species causing peaks A_0 and C_0 , the cyclic voltammogram of the isolated product
121 (**DIMP**) is shown in Figure 6. The cyclic voltammogram shows a pair of anodic and cathodic peaks at 0.16 and

122 0.11 V vs. Ag/AgCl, respectively, which are compatible with the potential of peaks A₀ and C₀. Accordingly, the
123 molecules that create peaks A₀ and C₀ and the redox behavior of them are shown in Figure 7.



124

125 **Figure 6.** Cyclic voltammogram of saturated solution of synthe sized product (**DIMP**) in coulometric conditions, at
126 room temperature.



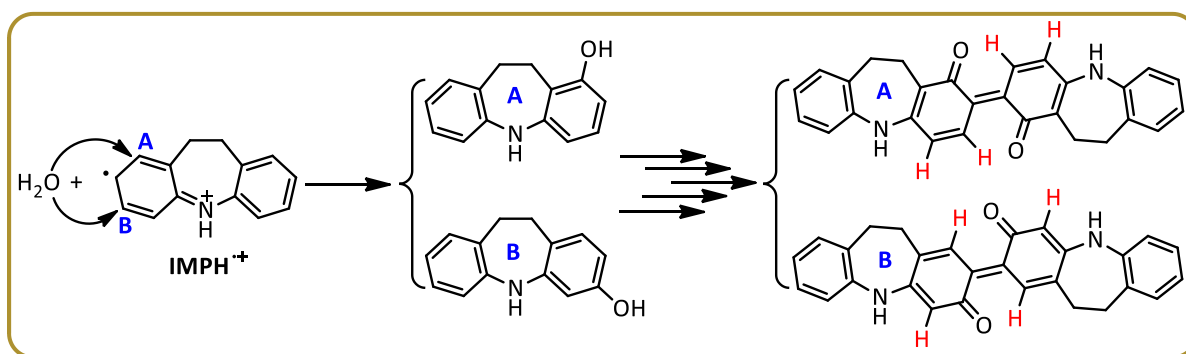
127

128 **Figure 7.** The redox behavior of A₀/C₀ peaks.

129 The second point that can be understood from this cyclic voltammogram is the presence of cathodic currents at
130 the beginning of the potential scan. These currents are related to the reduction of the compound present at the
131 electrode surface before the compound is oxidized at the potential of peak A₁. In other words, these currents
132 indicate that the product is in oxide form. These results are consistent with the structure of the **DIMP** which is in its
133 oxidized form.

134 An important point to note about hydroxylation of **IMPH⁺** is the location of the hydroxyl group in **IMPH-OH**
135 molecule.^{43,44} **IMPH⁺** can be attacked by water from two places A and B and become two different products
136 according to Fig. 4 (Figure 8). In the structures shown in Fig. 8, the hydrogens of the quinone rings have different

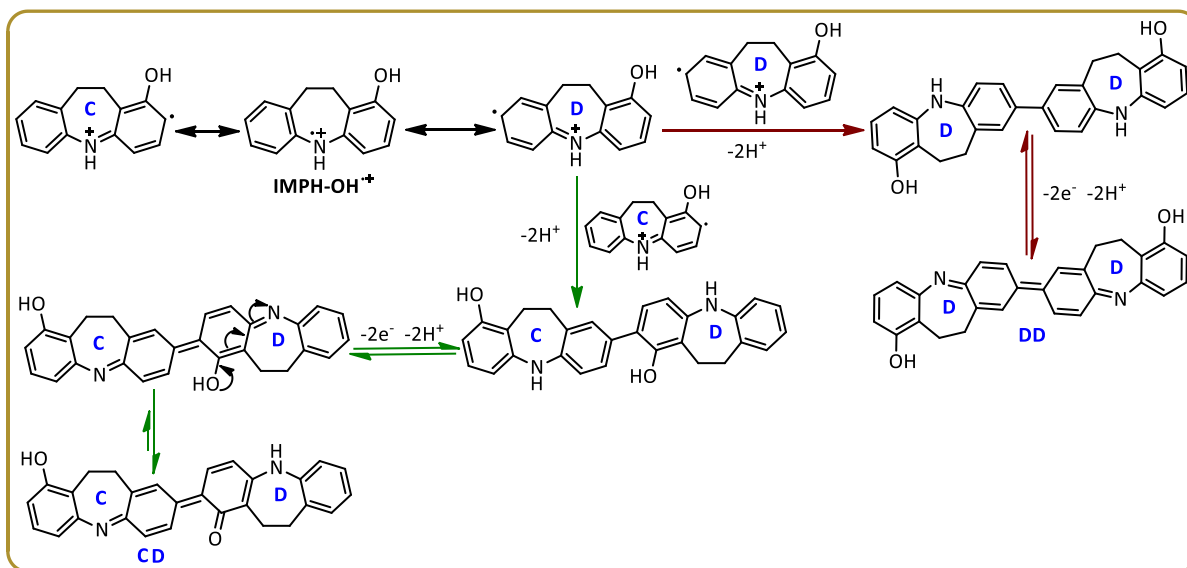
137 positions relative to each other. In structure A, the hydrogens of the quinone rings are in *ortho* positions, while in
 138 structure B, the hydrogens of the quinone rings are in *para* positions. We confirm the formation of structure A
 139 according to the results obtained from the NMR spectrum. The ^1H NMR spectrum of the reaction product (**DIMP**),
 140 shows clearly two doublet peaks with $J = 10$ and 8 Hz at $\delta 6.64$ and 7.64 ppm, respectively, showing coupling to
 141 the two *ortho* protons. These results are consistent with structure A.



142

143 **Figure 8.** Possible structures due to the increase of water to different positions of the **IMPH⁺** molecule.

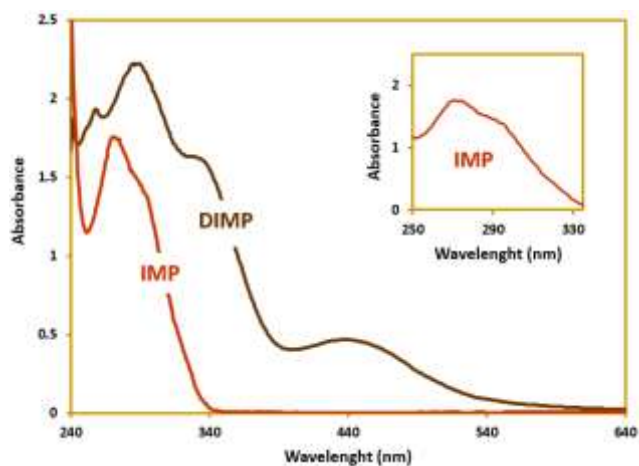
144 In addition, it is possible that the rearrangement of **IMPH-OH⁺** is preceded by different mechanisms and leads
 145 to the formation of a different products (**DD** and **CD**), as shown in Fig. 9. But we reject these mechanisms because
 146 of the results obtained from NMR spectra. As reported in the experimental section, the carbon NMR spectrum of
 147 the synthesized compound has a peak at 187.8 ppm, which corresponds to carbonyl groups, while the product, **DD**,
 148 shown in Fig. 9 has no carbonyl group. This finding causes us to reject the formation of **DD** product. On the other
 149 hand, the structure of the **CD** compound shows that this molecule is an asymmetric molecule, so that in its proton
 150 and carbon spectra, the number of peaks and their patterns are completely different from that of the synthesized
 151 product (**DIMP**). These findings rule out the formation of **CD** molecule as a final product.



152

153 **Figure 9.** Other mechanisms for the dimerization of **IMPH-OH**.

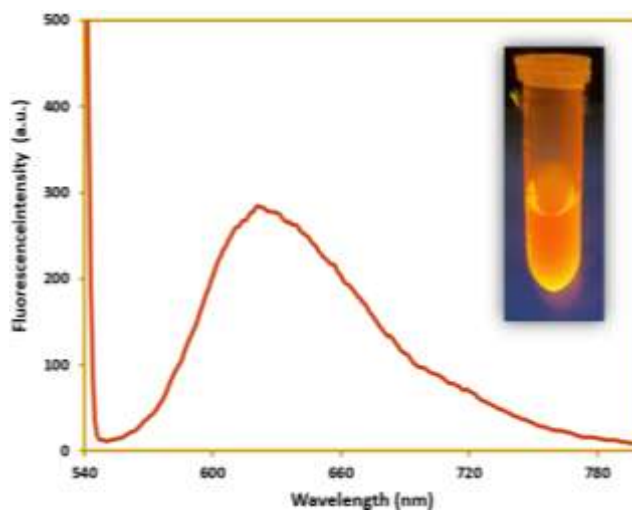
154 **UV-visible and fluorescence characteristics of DIMP.** In this part, spectrophotometric techniques were used to
 155 characterization of the ground state and the singlet excited state of synthesized product (**DIMP**) by means of
 156 absorption and fluorescence methods. Fig. 10 shows the UV-visible spectrum of 0.5 mM **IMP** and **DIMP** in
 157 chloroform. As can be seen, the absorption spectrum of **IMP** shows two bands at 270 and 295 nm were attributed to
 158 $\pi \rightarrow \pi^*$ transitions associated with the aromatic rings⁴⁵⁻⁴⁷ (Fig. 10, inset). A red shift was observed when the UV-
 159 visible spectrum has been carried out from **DIMP**, which can be related to the absence of the *N*-alkyl chain which
 160 has been replaced by hydrogen during electrochemical oxidation.⁴⁸ This result indicates that the alkyl chain-
 161 substituent affects the electronic transitions of the chromophore.⁴⁸ Also, the broad band from 400 to 520 nm with its
 162 maximum centered at 440 nm, is due to the conjugated double bonds.⁴⁵ The synthesized compound (**DIMP**) is
 163 colored (reddish yellow) and therefore may be used as a dye.⁴⁹⁻⁵¹ Based on this, the color quality of this compound
 164 has been evaluated and approved in the quality control laboratory of Alvan Sabet Company.



165

166 **Figure 10.** UV-visible spectra of **IMP** (0.5 mM) and **DIMP** (0.5 mM) in CHCl_3 . Inset: expanded **IMP**.

167 Fig. 11 shows the fluorescence spectrum of 0.5 mM **DIMP** in chloroform. For this experiment the fluorescence
 168 was monitored at an excitation wavelength of 535 nm at a 90° angle relative to the excitation light. Under these
 169 conditions, the emission wavelength of **DIMP** was found to be 625 nm. The conjugated bands in the structure of
 170 **DIMP** (Figure 4) caused to emergence of fluorescence properties in this compound.

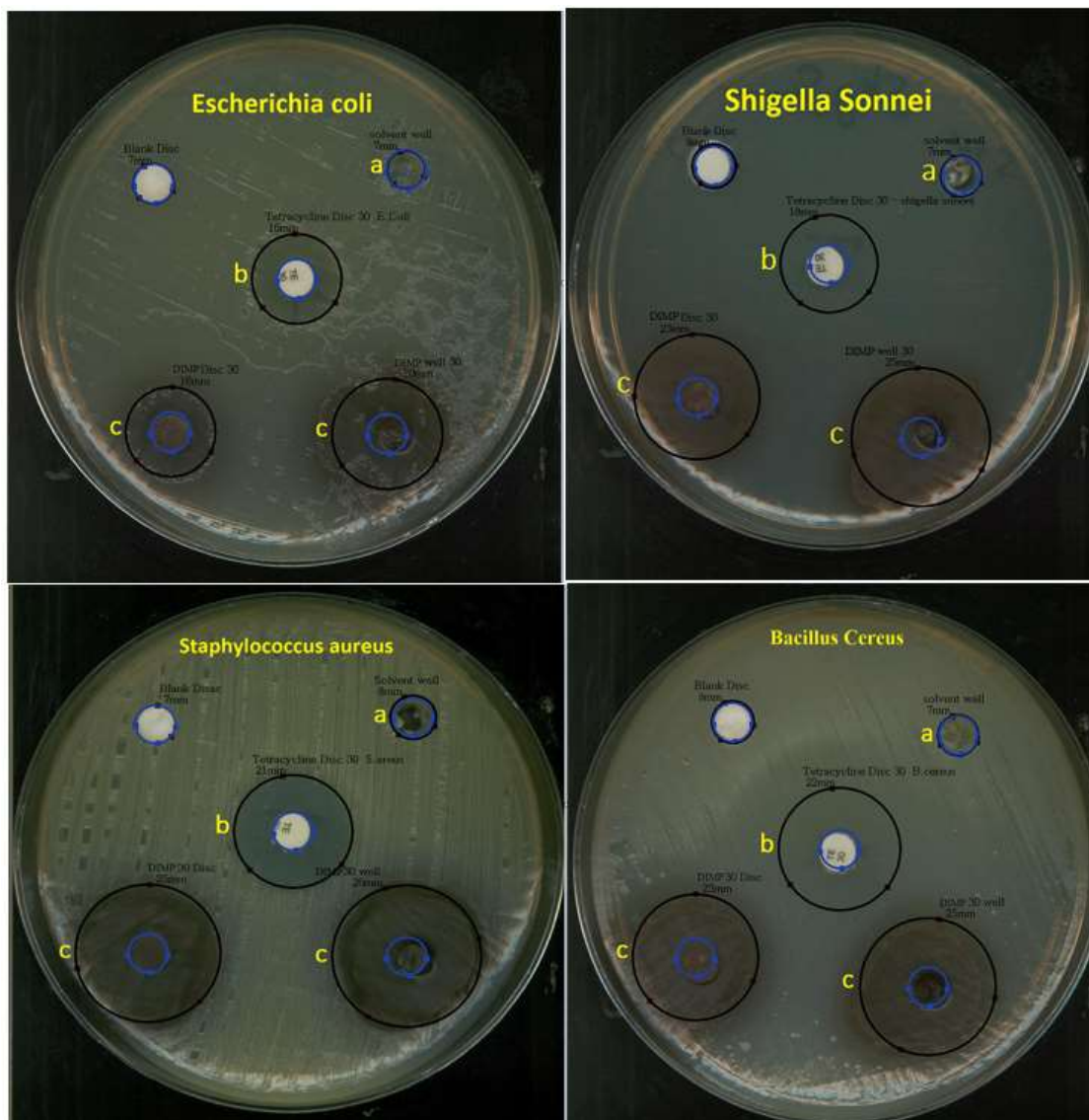


171

172 **Figure 11.** Fluorescent spectrum of **DIMP** and the photograph of **DIMP** (0.5 mM) using an ultraviolet lamp in
 173 CHCl_3 solvent measured under excitation of 535 nm.

174 **Antibacterial susceptibility.** The synthesized product **DIMP** was tested to evaluate the antibacterial activity. The
 175 effect of **DIMP** (30 mg ml^{-1}) on the four strains was assayed by agar well diffusion method and further confirmed
 176 by disk diffusion method. Four bacterial: *Bacillus cereus* (ATCC 14759), *Staphylococcus aureus* (ATCC 29213),

177 *Escherichia coli* (ATCC 25922) and *Shigella sonnei* (ATCC 9290) used in our study (Fig. 12). Antibiogram test
178 showed that the all gram positive and all gram negative bacteria (tested in this research) was sensitive to **DIMP**. For
179 determination of minimum inhibition concentrations (MIC) of the **DIMP** to inhibit the microorganisms more
180 studies are necessary and microdilution method is recommended. The result of antibacterial activity of the **DIMP**
181 compound is summarized in Table 1. These properties introduce **DIMP** as a fluorescent dye with antibacterial
182 activity.



183
184 **Figure 12.** Inhibition zone diameters (mm) obtained of *Bacillus cereus*, *Staphylococcus aureus*, *Escherichia coli*
185 and *Shigella sonnei* in disc diffusion test for 30 mg ml⁻¹ of (a) solvent, (b) tetracycline and (c) **DIMP**.

Name of the organisms	Solvent well	Blank disk	Tetracycline disc 30 µg	Well 30 µg	Disc 30µg	Activity
<i>Bacillus cereus</i>	-	-	22	25	23	(+)
<i>Staphylococcus aureus</i>	-	-	21	26	25	(+)
<i>Escherichia coli</i>	-	-	16	20	16	(+)
<i>Shigella sonnei</i>	-	-	18	25	23	(+)
<i>Bacillus cereus</i> ATCC 14759						Gram positive
<i>Staphylococcus aureus</i> ATCC 29213						Gram positive
<i>Escherichia coli</i> ATCC 25922						Gram negative
<i>Shigella sonnei</i> ATTC 9290						Gram negative

186 (+) Positive Activity, (-) Negative Activity, - No inhibition, Tetracycline = Standard drug
187 Solvent well = chloroform + Tween20

188 **Table 1.** Antibacterial activity of **DIMP** by agar well-diffusion method.

189 Conclusions

190 In this study, the electrochemical synthesis of **DIMP** is reported as a new derivative of dibenzazepine in good
191 yield and purity via C-C bond formation. To achieve this goal, the electrochemical behavior of **IMP** at different
192 temperatures was first investigated and it was found that the best pH value for the synthesis of **DIMP** is 5. The
193 results show that under these conditions, the oxidation of **IMP** proceeds through a complex path. It seems that the
194 first step in the synthesis of **DIMP** is oxidative dealkylation of **IMP**. After this step, a series of reactions,
195 including oxidation, hydroxylation, dimerization and oxidation, convert the dealkylated **IMP** to (*E*)-10,10',11,11'-
196 tetrahydro-[2,2'-bidibenzo[b,f] azepinylidene]-1,1'(5*H*,5'*H*)-dione (**DIMP**). The synthesis of **DIMP** is carried out
197 in the aqueous solution under mild conditions in one-pot without use of any toxic chemicals or organic solvents,
198 with a very simple procedure for separation and purification. The structure of **DIMP** is fully characterized by UV-
199 visible, FTIR, ¹H NMR, ¹³C NMR and mass spectrometry techniques. Conjugated double bonds in the structure of
200 **DIMP** cause the compound to become colored with sufficient fluorescence activity. In addition, the antibacterial
201 tests indicated that **DIMP** showed good antibacterial performance against all examined gram-positive and gram-
202 negative bacteria (*Staphylococcus aureus*, *Bacillus cereus*, *Escherichia coli* and *Shigella sonnei*). These properties
203 make the **DIMP** known as a unique fluorescent dye with antibacterial properties.

204

205 **Reagents and apparatus**

206 Cyclic voltammetry, controlled potential coulometry and macroscale electrolysis were performed using an
207 Autolab model PGSTAT 20 potentiostat/galvanostat. Absorption spectra was taken with a Lambda 25 UV-Vis
208 spectrophotometer. Fluorescence spectra was determined with a Varian spectrofluorometer. Both emission and
209 excitation bands were set at 5 nm. The working electrode used in the voltammetry experiments was a glassy
210 carbon disc (1.8 mm diameter) and a platinum wire was used as the counter electrode. The working electrode
211 used in controlled-potential coulometry and preparative electrolysis was an assembly of four ordinary soft
212 carbon rods (6 mm diameter and 4 cm length), while the counter electrode was a stainless-steel cylinder. The
213 working electrode potentials were measured versus Ag/AgCl (all electrodes from AZAR Electrodes).
214 Imipramine hydrochloride, 3-(10,11-dihydro-5*H*-dibenzo[*b,f*]azepin-5-yl)-*N,N*-dimethylpropan-1-aminium
215 chloride (C₁₉H₂₃N₂⁺Cl⁻) (Temad company, Iran), (MW = 280.407 g mol⁻¹ and M. p: 174-175°C) as the active
216 substance of imipramine was reagent-grade. Other chemicals were obtained from commercial source and used
217 without further purification.

218 **Electrochemical synthesis of DIMP**

219 Controlled-potential electrolysis was used as a preparative method for the synthesis of **DIMP**. Achieving this goal,
220 in an undivided cell equipped with carbon anode and stainless steel cathode, an aqueous solution (80 ml acetate
221 buffer, pH 5.0) containing **IMP** (0.25 mmol) was electrolyzed at potential of 0.85 V versus Ag/AgCl. Electrolysis
222 was discontinued when the current dropped to 5% of its initial value. Due to the fouling of electrode surface, the
223 electrolysis is sometimes stopped and the carbon anode was washed with acetone in order to reactivate it. At the end
224 of the electrolysis the cell was allowed to room temperature overnight. The precipitated solid was collected by
225 filtration and washed several times with water. The product was purified by thin layer chromatography (ethyl
226 acetate/*n*-hexane 50/50 v/v). After purification, product was characterized by UV-visible, IR, ¹H-NMR, ¹³C-NMR,
227 MS and melting point (M. p). Isolated yield: 75%. M. p: 138-139 °C, ¹H NMR (400 MHz, CHCl₃-*d*) δ 2.85 (t, 4H,
228 CH₂ aliphatic), 2.96 (t, 4H, CH₂ aliphatic), 6.31 (s, 2H), 6.64 (d, 2H, *J* = 10.0 Hz), 7.23 (d, 2H, *J* = 7.0 Hz), 7.29-
229 7.31 (m, 4H), 7.40 (t, 2H), 7.64 (d, 2H, *J* = 8.0 Hz). ¹³C NMR (100 MHz, CHCl₃-*d*) δ 31.5, 34.8, 127.9, 128.8,

230 129.7, 130.2, 130.5, 134.1, 135.0, 145.0, 146.0, 146.5, 155.1, 187.8. IR (KBr, cm⁻¹): 2924, 2855, 1741, 1642, 1615,
231 1593, 1489, 1350, 1293, 1155, 1089, 899, 817, 753, 668, 583. MS (EI, 70 eV): m/z (relative intensity): 420 (M+2H,
232 0.1), 243 (13.8), 209 (66.2), 180 (100), 152 (12.7), 128 (8.4), 109 (2.3), 89 (19.3), 63 (13.7), 43 (7.7).

233 **Antibacterial studies**

234 Agar well-diffusion method and disc diffusion method was followed to determine the antimicrobial activity of
235 **DIMP**. This material is melted in chloroform + Tween 20. The effect of **DIMP** 30 mg/ml on the four strains were
236 assayed by agar well diffusion method and further confirmed by disc diffusion method. Four bacterial ATCC strains
237 (*Bacillus cereus*, *Staphylococcus aureus*, *Escherichia coli*, *Shigella sonnei*) used in this study. The bacterial strains
238 were first incubated in brain heart infusion broth (BHI).^{52,53} After overnight incubation at 37°C, 10 µL of the broth
239 medium was streaked onto nutrient agar and then incubated for 24 h in the same condition. Then concentration of
240 bacterial, was balanced with a 0.5 McFarland standard. In agar well-diffusion method, Muller hinton agar (MHA)
241 plates were inoculated with bacteria and punched with a glass capillary to create well then filled with 30 mg each
242 the samples, Solvent well (chloroform + Tween20), blank disc and standard drug (tetracycline). The plates were
243 incubated at 37°C for 24 h. In disc diffusion method, Muller hinton agar (MHA) plates were inoculated with
244 bacteria then used discs prepared with 30 mg each the samples, Solvent disc (chloroform + Tween20), blank disc
245 and standard drug disc (tetracycline). The plates were incubated at 37°C for 24 h. Finally, the inhibition zone
246 surrounding the wells and disc were measured to evaluate of antibacterial activity.

247 **Acknowledgements**

248 The authors also acknowledge the Bu-Ali Sina and Yazd University Research Councils for their support of this work.

249 **Author information**

250 **Corresponding Author** * namat@basu.ac.ir , nematollahid@gmail.com

251 ORCID: Davood Nematollahi: 0000-0001-9638-224X

252 **Author contributions statement**

253 Z.S. and M.M.K.: methodology, validation, investigation, writing the original draft. D.N. writing-review & editing,
254 supervision, project administration. M.M.A.: supervision, resources. H.A. antibacterial experiments and
255 discussions.

256 **Additional information**

257 *Supplementary information* including FT-IR, ¹H NMR, ¹³C NMR, MS spectra of **DIMP** accompanies this paper at
258 <http://www.nature.com/srep>

259 **Competing financial interests:** The authors declare no competing financial and non-financial interests

260 **References**

- 261 1 Staub, K., Levina, G. A. & Fortd, A. Synthesis and stability studies of conformationally locked 4-
262 (diarylamino)aryl- and 4-(dialkylamino)phenyl-substituted second-order nonlinear optical polyene
263 chromophores. *J. Mater. Chem.* **13**, 825–833 (2003).
- 264 2 Wang, Y. *et al.* Influence of the donor size in panchromatic D–π–A–π–A dyes bearing 5-phenyl-5H-dibenzo-
265 [b,f]azepine units for dye-sensitized solar cells. *Dyes Pigm.* **127**, 204–212 (2016).
- 266 3 Datar, P. A. Quantitative bioanalytical and analytical method development of dibenzazepine derivative,
267 carbamazepine: A review. *J. Pharm. Anal.* **5**, 213–222 (2015).
- 268 4 Thiele, J. & Holzinger, O. Properties of *o*-diaminodibenzyl. *Liebigs Ann. Chem.* **305**, 96–102 (1899).
- 269 5 Schindler, W. & Häfliger, F. Derivatives of iminodibenzyl. *Helv. Chim. Acta* **37**, 472–83 (1954).
- 270 6 Tsai, Y. L., Chang, C. C., Kang, C. C. & Chang, T. C. Effect of different electronic properties on 9-aryl-
271 substituted BMVC derivatives for new fluorescence probes. *J. Lumin.* **127**, 41–47 (2007).
- 272 7 Li, W., Qiao, J., Duan, L., Wang, L. D. & Qiu, Y. Novel fluorene/carbazole hybrids with steric bulk as host
273 materials for blue organic electrophosphorescent devices. *Tetrahedron* **63**, 10161–10168 (2007).
- 274 8 Yoon, K. R., Ko, S. O., Lee, S. M. & Lee, H. Synthesis and characterization of carbazole derived nonlinear
275 optical dyes. *Dye Pigm.* **75**, 567–573 (2007).
- 276 9 Lu, Q. *et al.* Novel polyamides with 5H-dibenzo [b,f] azepin-5-yl-substituted triphenylamine: Synthesis and
277 visible-NIR electrochromic properties. *Polymers* **9**, 542–562 (2017).
- 278 10 Zhou, Y. H., Peng, P., Han, L. & Tian, W. J. Novel donor–acceptor molecules as donors for bulk
279 heterojunction solar cells. *Synth. Met.* **157**, 502–507 (2007).
- 280 11 Wang, Y. *et al.* Influence of the donor size in panchromatic D–π–A–π–A dyes bearing 5-phenyl-5H-dibenzo-
281 [b,f]azepine units for dye-sensitized solar cells. *Dyes Pigm.* **127**, 204–212 (2016).

- 282 12 Li, X. H. *et al.* A new carbazole-based phenanthrenyl ruthenium complex as sensitizer for a dye-sensitized
283 solar cell. *Inorg. Chim. Acta* **361**, 2835–2840 (2008).
- 284 13 Tang, Y. Z. & Liu, Z. Q. Free-radical-scavenging effect of carbazole derivatives on AAPH-induced hemolysis
285 of human erythrocytes. *Bioorg. Med. Chem.* **15**, 1903-1913 (2007).
- 286 14 Balaure, P. C., Costea, I., Iordache, F., Drăghici, C. & Enache, C. Synthesis of New dibenzo[b,f]azepine
287 derivatives. *Rev. Roum. Chim.* **54**, 935-942 (2009).
- 288 15 Kricka, L. J. & Ledwith, A. Dibenz[b,f]azepines and related ring systems. *Chem. Rev.* **74**, 101-123 (1974).
- 289 16 Knell, A., Monti, D., Maciejewski, M. & Baiker, A. Catalytic dehydrogenation of 10,11-dihydro-5H-dibenz
290 [b,f]azepine (iminodibenzyl) to 5H-dibenz[b,f]azepine (iminostilbene) over potassium-promoted iron
291 oxides: Effect of steam, potassium promotion and carbon dioxide treatment. *Appl. Catal. A* **124**, 367-390
292 (1995).
- 293 17 Elliott, E. C. *et al.* Convenient syntheses of benzo-fluorinated dibenz[b,f]azepines: Rearrangements of
294 isatins, acridines, and indoles. *Org. Lett.* **13**, 5592-5595 (2011).
- 295 18 Zhang, X., Yang, Y. & Liang, Y. Palladium-catalyzed double *N*-arylation to synthesize multisubstituted
296 dibenzoazepine derivatives. *Tetrahedron Lett.* **53**, 6406-6408 (2012).
- 297 19 Tselikhovsky, D. & Buchwald, S. L. Synthesis of heterocycles via Pd-Ligand controlled cyclization of 2-
298 Chloro-*N*-(2-vinyl) aniline: Preparation of carbazoles, indoles, dibenzazepines, and acridines. *J. Am. Chem.*
299 *Soc.* **132**, 14048-14051 (2010).
- 300 20 Modha, S. G., Vachhani, D. D., Jacobs, J., Van Meervelt, L. & Van der Eycken, E. V. A concise route to
301 indoloazocines via a sequential Ugi–gold-catalyzed intramolecular hydroarylation. *Chem Comm.* **48**, 6550-
302 6552 (2012).
- 303 21 Ito, M., Takaki, A., Okamura, M., Kanyiva, K. S. & Shibata, T. Catalytic synthesis of dibenzazepines and
304 dibenzazocines by 7-exo-and 8-endo-dig-selective cycloisomerization. *Eur. J. Org. Chem.* **2021**, 1688-1692
305 (2021).
- 306 22 Romero, K. J., Galliher, M. S., Pratt, D. A. & Stephenson, C. R. Radicals in natural product synthesis. *Chem.*
307 *Soc. Rev.* **47**, 7851-7866 (2018).
- 308 23 Lotfi, S., Tammari, E. & Nezhadali, A. Mechanistic study of in vitro chemical interaction of trimipramine
309 drug with barbituric derivative after its oxidation: Electrochemical synthesis of new dibenzazepine
310 derivative. *Mater. Sci. Eng. C* **76**, 153-160 (2017).
- 311 24 Xiong, P., Xu, H. H., Song, J. & Xu, H. C. Electrochemical difluoromethylarylation of alkynes. *J. Am. Chem.*
312 *Soc.* **140**, 2460-2464 (2018).
- 313 25 Martins, G. M., Shirinfar, B., Hardwick, T., Murtaza, A. & Ahmed, N. Organic electrosynthesis:
314 electrochemical alkyne functionalization. *Catal. Sci. Technol.* **9**, 5868-5881 (2019).
- 315 26 Tammari, E., Nezhadali, A. & Lotfi, S. Electrochemical oxidation of desipramine drug in the presence of 4,
316 6-dimethylpyrimidine-2-thiol nucleophile in aqueous acidic medium. *Electroanalysis* **27**, 1693-1698 (2015).
- 317 27 Momeni, S. & Nematollahi, D. Electrosynthesis of new quinone sulfonimide derivatives using a
318 conventional batch and a new electrolyte-free flow cell. *Green Chem.* **20**, 4036-4042 (2018).

- 319 28 Goljani, H., Tavakkoli, Z., Sadatnabi, A. & Nematollahi, D. Two-phase electrochemical generation of
320 aryldiazonium salts: Application in electrogenerated copper-catalyzed sandmeyer reactions. *Org. Lett.* **22**,
321 5920-5924 (2020).
- 322 29 Goljani, H., Tavakkoli, Z., Sadatnabi, A., Masoudi-Khoram, M. & Nematollahi, D. A new electrochemical
323 strategy for the synthesis of a new type of sulfonamide derivatives. *Sci. Rep.* **10**, 1-10 (2020).
- 324 30 Masoudi-Khoram, M., Nematollahi, D., Jamshidi, M. & Goljani, H. Electrochemical study of fast blue BB. A
325 green strategy for sulfinatation of fast blue BB. *New J. Chem.* **43**, 10382-10389 (2019).
- 326 31 Zivari-Moshfegh, F., Nematollahi, D., Masoudi-Khoram, M. & Rahimi, A. Electrochemical oxidation of *o*-
327 phenylenediamine and 1,3 dihydrospiro[benzo[d] imidazole-2,1'-cyclohexane]. A comprehensive study
328 and introducing a novel case of *CE* mechanism. *Electrochim. Acta* **354**, 136700 (2020).
- 329 32 Masoudi-Khoram, M., Nematollahi, D., Khazalpour, S., Momeni, S. & Jamshidi, M. Comparative evaluation
330 of the efficiency of batch and flow electrochemical cells in the synthesis of a new derivative of 2-
331 thenoyltrifluoroacetone. *J. Electroanal. Chem.* **879**, 114796 (2020).
- 332 33 Youseflooie, N., Alizadeh, S., Masoudi-Khoram, M., Nematollahi, D. & Alizadeh, H. A comprehensive
333 electrochemical study of 2-mercaptobenzoheterocyclic derivatives. Air-assisted electrochemical synthesis
334 of new sulfonamide derivatives. *Electrochim. Acta* **353**, 136451 (2020).
- 335 34 Meyer, T. H., Choi, I., Tian, C. & Ackermann, L. Powering the future: how can electrochemistry make a
336 difference in organic synthesis? *Chem.* **6**, 2484–2496 (2020).
- 337 35 De Toledo, R. A. *et al.* Use of graphite polyurethane composite electrode for imipramine oxidation—
338 mechanism proposal and electroanalytical determination. *Anal. Lett.* **39**, 507-520 (2006).
- 339 36 Sanghavi, B. J. & Srivastava, A. K. Adsorptive stripping voltammetric determination of imipramine,
340 trimipramine and desipramine employing titanium dioxide nanoparticles and an Amberlite XAD-2
341 modified glassy carbon paste electrode. *Analyst* **138**, 1395-1404 (2013).
- 342 37 Wiśniewska, J., Wrzeszcz, G., Kurzawa, M. & van Eldik, R. The oxidative degradation of dibenzoazepine
343 derivatives by cerium (IV) complexes in acidic sulfate media. *Dalton Trans.* **41**, 1259-1267 (2012).
- 344 38 Bishop, E. & Hussein, W. Electroanalytical study of tricyclic antidepressants. *Analyst* **109**, 73–80 (1984).
- 345 39 Martinez, M. A., Sánchez de la Torre, C. & Almarza, E. A comparative solid-phase extraction study for the
346 simultaneous determination of fluoxetine, amitriptyline, nortriptyline, trimipramine, maprotiline,
347 clomipramine and trazodone in whole blood by capillary gas-liquid chromatography with nitrogen-
348 phosphorus detection. *J. Anal. Toxicol.* **27**, 353–358 (2003).
- 349 40 Soury, Z., Ansari, A., Nematollahi, D. & Mazloum-Ardakani, M. Electrocatalytic degradation of
350 dibenzoazepine drugs by fluorine doped β -PbO₂ electrode: New insight into the electrochemical oxidation
351 and mineralization mechanisms. *J. Electroanal. Chem.* **862**, 114037 (2020).
- 352 41 Soury, Z., Alizadeh, S., Nematollahi, D., Mazloum-Ardakani, M. & Karami, A. A green and template-free
353 electropolymerization of imipramine. The decoration of sponge-like polymer film with gold nanoparticles.
354 *J. Electroanal. Chem.* **894**, 115340 (2021).

355 42 Masui, M. & Sayo, H. Anodic oxidation of amines. Part II. Electrochemical dealkylation of aliphatic tertiary
356 amines. *J. Chem. Soc. B* 1593-1596 (1971).

357 43 Eberhardt, M. K. Reaction of benzene radical cation with water. Evidence for the reversibility of hydroxyl
358 radical addition to benzene. *J. Am. Chem. Soc.* **103**, 3876-3878 (1981).

359 44 Eberhardt, M. K. Radiation-induced homolytic aromatic substitution. 6. The effect of metal ions on the
360 hydroxylation of benzonitrile, anisole, and fluorobenzene. *J. Phys. Chem.* **81**, 1051-1057 (1977).

361 45 Niu, H. *et al.*, Simple approach to regulate the spectra of novel kinds of polyazomethines containing bulky
362 triphenylamine: Electrochemistry, electrochromism and photophysical responsive to environment. *Dyes*
363 *Pigm.* **96**, 158-169 (2013).

364 46 Lu, Q. *et al.*, Novel polyamides with 5*H*-dibenzo [b,f] azepin-5-yl-substituted triphenylamine: Synthesis and
365 visible-NIR electrochromic properties. *Polymers* **9**, 542-562 (2017).

366 47 Azadbakht, R., Koolivand, M. & Menati, S. Salicylimine-based fluorescent chemosensor for magnesium
367 ions in aqueous solution. *Inorganica Chim. Acta* **514**, 120021 (2021).

368 48 García, C., Oyola, R., Piñero, L., Hernández, D. & Arce, R. Photophysics and photochemistry of imipramine,
369 desimipramine, and clomipramine in several solvents: a fluorescence, 266 nm laser flash, and theoretical
370 study. *J. Phys. Chem. B* **112**, 168-178 (2008).

371 49 Liu, X. *et al.*, Effect of structural modification on the performances of phenothiazine-dye sensitized solar
372 cells. *Dyes Pigm.* **121**, 118-127 (2015).

373 50 Shaki, H., Gharanjig, K., Rouhani, S. & Khosravi, A. Synthesis and photophysical properties of some novel
374 fluorescent dyes based on naphthalimide derivatives. *J. Photochem. Photobiol. A* **216**, 44-50 (2010).

375 51 Hosseinnezhad, M. & Rouhani, S. Synthesis and application of new fluorescent dyes in dye-sensitized solar
376 cells. *Appl. Phys. A* **123**, 1-10 (2017).

377 52 Bonev, B., Hooper, J. & Parisot, J. Principles of assessing bacterial susceptibility to antibiotics using the
378 agar diffusion method. *J. Antimicrob. Chemother.* **61**, 1295-1301 (2008).

379 53 Rex, J. H. *et al.*, Development of interpretive breakpoints for antifungal susceptibility testing: conceptual
380 framework and analysis of in vitro-in vivo correlation data for fluconazole, itraconazole, and candida
381 infections. *Clin. Infect. Dis.* **24**, 235-247 (1997).

382

383

Supplementary Files

This is a list of supplementary files associated with this preprint. Click to download.

- [SI.docx](#)